

Northumbria Research Link

Citation: Mirzaei, Mohammad Amin, Zare Oskouei, Morteza, Mohammadi-Ivatloo, Behnam, Loni, Abdolah, Zare, Kazem, Marzband, Mousa and Shafiee, Mahmood (2020) Integrated energy hub system based on power-to-gas and compressed air energy storage technologies in the presence of multiple shiftable loads. IET Generation, Transmission & Distribution, 14 (13). pp. 2510-2519. ISSN 1751-8687

Published by: IET

URL: <https://doi.org/10.1049/iet-gtd.2019.1163> <<https://doi.org/10.1049/iet-gtd.2019.1163>>

This version was downloaded from Northumbria Research Link: <http://nrl.northumbria.ac.uk/id/eprint/43150/>

Northumbria University has developed Northumbria Research Link (NRL) to enable users to access the University's research output. Copyright © and moral rights for items on NRL are retained by the individual author(s) and/or other copyright owners. Single copies of full items can be reproduced, displayed or performed, and given to third parties in any format or medium for personal research or study, educational, or not-for-profit purposes without prior permission or charge, provided the authors, title and full bibliographic details are given, as well as a hyperlink and/or URL to the original metadata page. The content must not be changed in any way. Full items must not be sold commercially in any format or medium without formal permission of the copyright holder. The full policy is available online: <http://nrl.northumbria.ac.uk/policies.html>

This document may differ from the final, published version of the research and has been made available online in accordance with publisher policies. To read and/or cite from the published version of the research, please visit the publisher's website (a subscription may be required.)

An Integrated Energy Hub System based on Power-to-Gas and Compressed Air Energy Storage Technologies in presence of Multiple Shiftable Loads

Mohammad Amin Mirzaei¹, Morteza Zare Oskouei¹, Behnam Mohammadi-ivatloo^{1*}, Abdollah Loni², Kazem Zare¹, Mousa Marzband², Mahmood Shafiee³

¹ Smart Energy Systems Laboratory, Faculty of Electrical and Computer Engineering, University of Tabriz, Tabriz, Iran

² Department of Mechanical and Electrical Engineering, Northumbria University, Newcastle, UK

³ School of Engineering and Digital Arts, University of Kent, Canterbury, UK

* E-mail: bmohammadi@tabrizu.ac.ir

Abstract: Integrated energy carriers in the framework of energy hub system (EHS) have an undeniable role in reducing operating cost and increasing energy efficiency as well as system's reliability. Nowadays, Power-to-Gas (P2G), as a novel technology, is a great choice to intensify the interdependency between electricity and natural gas networks. The proposed strategy of this paper is divided into three parts: (i) a stochastic model is presented to determine the optimal day-ahead scheduling of the EHS with the coordinated operating of P2G storage and tri-state Compressed Air Energy Storage (CAES) system. The main objective of the proposed strategy is to indicate the positive impact of P2G storage and tri-state CAES on lessening the uncertainty derived from renewable sources and the operating cost of EHS, including: Combined Heat and Power (CHP), heat storage system, gas boiler (GB), and wind turbine that would meet the demands of electrical, gas, and thermal. Also, the uncertainty of electricity market price, power generation of the wind turbine, and even electrical, gas, and thermal demands are considered. (ii) A demand response program (DRP) focusing on day-ahead load shifting is applied on the multiple electrical loads according to the load's activity schedule. (iii) the Conditional Value-at-Risk (CVaR) algorithm, as a risk measure technique, is utilized with the proposed strategy to evaluate the risk-aversion of the EHS's operator. The proposed strategy is successfully applied to an illustrative example and is solved by GAMS software. The obtained results validate the proposed strategy by demonstrating the considerable diminution in operating cost of the EHS by almost 4.5%.

Nomenclature

Acronyms

| | |
|------|------------------------------------|
| CAES | Compressed air energy storage. |
| CHP | Combined heat and power. |
| CVaR | Conditional value-at-risk. |
| DRP | Demand response program. |
| EHS | Energy hub system. |
| GAMS | General algebraic modeling system. |
| GB | Gas boiler. |
| MIP | Mixed integer programming. |
| P2G | Power-to-gas. |

Indices

| | |
|------|--------------------|
| b | Gas boiler. |
| c | Charging mode. |
| d | Discharging mode. |
| hs | Heat storage. |
| i | CHP unit. |
| k | CAES system. |
| m | Active load. |
| pg | P2G storage. |
| s | Scenario. |
| si | Simple cycle mode. |
| t | Time interval. |

Parameters

| | |
|-----|-----------------------------|
| NT | Total scheduling period. |
| NI | Total CHP units. |
| NK | Total CAES systems. |
| NHS | Total heat storage systems. |
| NB | Total gas boiler units. |
| NS | Total scenarios. |

| | |
|------------------------------------|--|
| VOM^{Exp}, VOM^C | Variable operation cost of expander/compressor of CAES system. |
| $\lambda_{t,s}^e$ | Power price. |
| $\lambda_{t,s}^g$ | Gas price. |
| $A^{k,max}, A^{k,min}$ | Max/Min energy capacity of CAES system. |
| $B^{hs,max}, B^{hs,min}$ | Max/Min capacity of heat storage. |
| $B^{hs}(\cdot), max$ | Maximum charge/discharge rate of heat storage. |
| $DL_{t,s}$ | Electrical demand. |
| $DR_{m,t,s}$ | Adjustable load value of active loads. |
| $GL_{t,s}$ | Gas demand. |
| $G^{pg}(\cdot), max$ | Maximum stored/supplied gas by P2G storage. |
| $GT^{B,max}, GT^{S,max}$ | Maximum exchanged gas energy. |
| $H^{b,max}, H^{b,min}$ | Max/Min capacity of gas boiler. |
| $HL_{t,s}$ | Heat demand. |
| Inc_m | Incentive cost of active shiftable loads. |
| $P^{i,max}, P^{i,min}$ | Max/Min generated power of CHP unit. |
| $P^{k,c,max}, P^{k,c,min}$ | Max/Min charge capacity of CAES system. |
| $P^{k,d,max}, P^{k,d,min}$ | Max/Min discharge capacity of CAES system. |
| $P^{k,si,max}, P^{k,si,min}$ | Max/Min capacity of CAES system in simple cycle mode. |
| ppg,max | Maximum consumed power by P2G storage. |
| $PL^{B,max}, PL^{S,max}$ | Maximum exchanged power. |
| $R^{i,up}, R^{i,dn}$ | Up/Down ramp rate limit of CHP unit. |
| $SU_{t,s}(\cdot), SD_{t,s}(\cdot)$ | Start-up and shut-down fuel consumption. |
| $T^{i,ON}, T^{i,OFF}$ | Minimum on/off time interval of CHP unit. |
| UT^i, DT^i | Minimum up and down time of CHP unit. |
| $V^{pg,max}, V^{pg,min}$ | Max/Min capacity of P2G storage. |

| | |
|---|--|
| $\eta^{hs}, \eta^{hs,c}, \eta^{hs,d}$ | The efficiency of heat storage in Standby/charge/discharge. |
| $\eta^{k,c}, \eta^{k,d}, \eta^{k,si}$ | The efficiency of CAES system in Charge/discharge/simple cycle mode. |
| $\eta^i, \eta^b, \eta^{pg}$ | The efficiency of CHP unit, gas boiler, P2G storage. |
| π_s | Probability of scenarios. |
| β | Risk factor. |
| Decision Variables | |
| $A_{t,s}^k$ | The energy level of CAES system. |
| $B_{t,s}^{hs}$ | The energy level of heat storage. |
| $d_{t,s}^{DR}$ | Electrical load after implementation of DRP. |
| $dr_{m,t,s}^{up}, dr_{m,t,s}^{dn}$ | Electrical load change after implementation of load shifting program. |
| $EL_{t,s}^+, EL_{t,s}^-$ | Bought/sold power from/to upstream power network. |
| $G_{t,s}^{pg,c}$ | The gas stored by P2G storage. |
| $G_{t,s}^{pg,d}$ | The gas supplied by P2G storage. |
| $GE_{t,s}^{pg}$ | The gas produced by P2G storage. |
| $GB_{t,s}^b$ | The gas consumed by gas boiler. |
| $GC_{t,s}^i$ | The gas consumed by CHP unit. |
| $GK_{t,s}^k$ | The gas consumed by CAES system. |
| $GM_{t,s}^+, GM_{t,s}^-$ | Bought/sold gas from/to upstream gas network. |
| $H_{t,s}^i$ | The generated heat by CHP unit. |
| $H_{t,s}^b$ | The generated heat by gas boiler. |
| $H_{t,s}^{hs,d}$ | Heat supplied by heat storage. |
| $H_{t,s}^{hs,c}$ | Heat stored by heat storage. |
| $P_{t,s}^i$ | Generated power by CHP unit. |
| $PW_{t,s}$ | Generated wind power. |
| $P_{t,s}^{pg}$ | Power consumed by P2G storage. |
| $P_{t,s}^{k,si}, P_{t,s}^{k,d}$ | Generated power in simple cycle/discharge mode by CAES system. |
| $P_{t,s}^{k,c}$ | Consumed power in charge mode by CAES. |
| $V_{t,s}^{pg}$ | The energy level of P2G storage. |
| M | Positive constant. |
| $I_{t,s}^{(\cdot)}, Y_{t,s}^i, Z_{t,s}^i$ | Binary variables to indicate the status of different equipment. |
| $e_{t,s}^{(\cdot)}, g_{t,s}^{(\cdot)}$ | Binary variables to indicate bought/sold energy from/to upstream networks. |

1 Introduction

Nowadays, the use of natural gas as an alternative source for coal and nuclear fuels is an ideal solution to supply electrical demands in three energy sectors of residential, commercial, and industrial. Various technical methods have been developed to optimally integrate natural gas networks with the electricity grid and increase energy efficiency in electrical systems [1]. The main approach of these methods is to create a suitable platform based on different multi-stage optimization programs to optimize the energy flow in the integrated systems [2–4]. Establishing an appropriate connection between electricity and natural gas networks brings many benefits to society (such as reducing the greenhouse gas emissions), consumers (such as decreasing energy price), and grid operators (such as boosting the power system reliability) [5–7]. For this reason, in recent years, the energy hub system (EHS) as an emerging concept has been utilized to supply the demands of electrical, thermal, and gas [8]. Conversion facilities and up-to-date energy storage technologies in the EHS have an important role to fulfill the various demands of consumers via creating an optimal connection between electricity and gas networks. To increase the efficiency and decrease the operating cost of the EHS, making the use of advanced technologies like Power-to-Gas (P2G) storage and tri-state Compressed Air Energy Storage (CAES) system is essential [9–13]. The tri-state refers to three CAES modes including charge, discharge, and simple

cycle. Utilizing the CAES in the simple cycle mode in coordination with P2G enables more efficient exploitation of the gas network and improves the interdependencies between electricity and natural gas networks in the EHS. This combined operation scheme provides significant arbitrage opportunities by converting electrical energy into natural gas during low-electrical price hours. Also, it provides the electric power generation of the natural gas network at low-gas price hours [14]. Furthermore, the use of CAES in comparison with other electrical storage systems has many advantages for the EHS's operator such as (i) storing a large amount of energy, (ii) unlike pumped hydroelectric storage, it does not need to specific location for installation, and (iii) agility-wise (quick response to possible changes in pressure times) [15].

As stated in the literature, the optimization of EHS operation in the day-ahead market with consideration of different equipment has attracted much attention from the researchers' perspective. The optimization frameworks have been modelled based on several different aspects in the EHS. The main objectives of the proposed structures are: (i) reducing the total operating cost [16], (ii) increasing the penetration of renewable energy sources [17], (iii) supplying the various energy demands [18], (iv) applying different approaches to modelling the stochastic programming [19, 20], and (v) executing demand response programs (DRPs) aiming at reducing the consumers' bill [21].

According to the abovementioned aspects, numerous works have investigated the challenges associated with the EHS operation. Mainly, the shortcomings (**Sh**) of the existing literature are summarized as follows:

Sh1: the optimal scheduling of the EHS has been investigated in [22–24], considering the various equipment and different uncertainty methodologies. In these studies, the short-term EHS scheduling for multiple energy networks consisting of electricity and natural gas have been studied to reduce or compensate the uncertainty in the wind power generation and/or electrical demand. Furthermore, in [25, 26], the total system's cost minimization in the multi-carrier energy systems has been followed up considering uncertainties regarding electrical demand, and day-ahead electricity market prices. Nevertheless,

(i) the effect of the P2G storage was not considered in the above-mentioned studies to determine the proper operation of the EHS, compensate the uncertainty in the output power of renewable resources, and decrease the day-ahead operating cost.

(ii) the benefits of tri-state CAES were ignored in the reviewed literature, as the efficient storage device that has the potential to affect the operating cost of the EHS.

(iii) the uncertainties of electrical, gas, and thermal demands were not estimated in presented approaches in [25, 26], and

(iv) the impact of gas demand on the optimality of the results was not studied in [22, 23].

Sh2: DRPs have been implemented in [27–29] to meet the energy demands in the EHS. In these works, the main concern is to decrease the effect of various variable uncertainties associated with the distributed power generation systems and electrical demands on the optimal operation of the EHS by utilizing DRPs. Also, Time-Based Rate Programs (TBRPs) as the major demand response techniques have been implemented in the electrical demands of the EHS to achieve the desired goals. But, the impact of customer satisfaction was not taken into account for DRPs in any of the aforementioned papers.

To tackle the mentioned issues, this paper proposes a comprehensive EHS based on P2G storage and tri-CAES system. Also, the Conditional Value-at-Risk (CVaR) methodology is utilized to quantify the potential risk of the EHS scheduling problem. The proposed model schedules an integrated EHS with considering CHP unit, heat storage system, gas boiler (GB) unit, and wind turbine in the presence of load shifting technique. The load activity schedule is utilized for load shifting program according to customer satisfaction. Besides heating and electrical demands, gas demands are considered. For achieving more accurate results, the uncertainties derived from electricity market price, power generation of the wind turbine, and electrical, gas and thermal demands are estimated. In general, the main contributions (**C**) of this paper can be listed as follows:

C1: Proposing integrated EHS with P2G storage and tri-CAES system to reduce the total operating cost of the EHS and compensate the uncertainty in the output power of wind turbine, electricity, heat and gas demands (Tackled **Sh1**).

C2: Implementing DRPs based on load shifting to reduce the operating cost of the EHS, considering the multiple electrical loads' activity schedule including residential, commercial, and industrial (Tackled **Sh2**).

The remaining parts of this paper are organized as follows: Section 2 presents the structure of the proposed model in this study. The mathematical formulation and constraints regarding the optimal scheduling of EHS are provided in Section 3. Section 4 presents simulation results and discussions on the obtained results. Finally, the conclusions are presented in Section 5.

2 Description of Proposed Framework

2.1 P2G Concept

The P2G storage makes the use of electricity to split water into hydrogen and oxygen via electrolysis, which can be described by $2H_2O \rightarrow 2H_2 + O_2$. This emerging technology may be Alkaline Electrolysis (AE) or Proton Exchange Membrane (PEM). The produced hydrogen interacts with carbon dioxide by means of Sabatier reaction, which results in Synthetic Natural Gas (SNG): $CO_2 + 4H_2 \rightarrow CH_4 + 2H_2O$. This progress may be either chemical or biological. In Fig. 1, these two processes represent the major steps in developing the P2G technology. The overall energy conversion efficiency of a traditional P2G technology ranges between 50% and 60%. By increasing the energy conversion efficiency of P2G storage to 85%, P2G facilities can carry out cross-commodity arbitrage trade between electricity and natural gas markets aimed to lessen the operating cost of EHS [30]. When the price gap between electric energy and natural gas prices is remarkable in order to cover conversion losses, the EHS operator can profit from converting power to gas. Especially, the power to hydrogen (P2H) in the first stage is more efficient than the whole P2G process. Although, P2G storage offers several advantages over P2H, but the utilization of hydrogen is limited to fuel cells in certain industries. The produced SNG by P2G has more extensive applications and can be consumed by gas-fired units, which raises the operation flexibility of the two facilities. On the other hand, SNG has similar properties to Conventional Natural Gas (CNG) and thus can be stored, transmitted and traded in natural gas system. However, there are technical and legislative restrictions on the quantity of H_2 that may be injected into the natural gas network. Therefore, SNG is more realistic in prevailing conditions and P2G technology is considered in this paper.

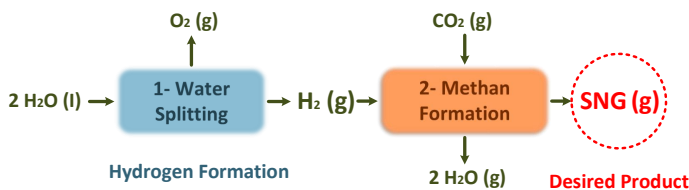


Fig. 1: CH_4 formation mechanism by P2G pathway

2.2 CAES Concept

Nowadays, the use of CAES is becoming popular in comparison with other energy storage systems. The reason for this popularity is that the CAES does not require a specific geographic location for installation compared to a pumped storage plant. Therefore, it can be installed and used in an unrestricted electrical network. In addition, CAES has a lower investment cost compared to the pumped storage plants [31]. Against other energy storage technologies, CAES is more appropriate for producing and storing high-capacity power. On the other hand, CAES has a very high rate of flexibility. For instance,

the 110 MW McIntosh Power Plant with a productive capacity of 134 MW and a compressive strength of 110 MW can change from complete production to complete compression in less than five minutes [32]. Another advantage of the CAES is that it works in three modes including charging, discharging, and simple cycle. Moreover, it can generate power exactly like a gas-fired power plant. This technology compresses air when the electricity price is low. Then, the compressed air is stored in a salty dome-shaped space. In times of high electricity prices, this system can make the use of compressed air to generate electricity. Hence, there is no need for extra gas to compress air. Therefore, with regard to the features mentioned, CAES can be considered as an alternative option for the hub operator to reduce the operating cost of EHS. Fig. 2 depicts the procedure of energy generation by a simple type of CAES.

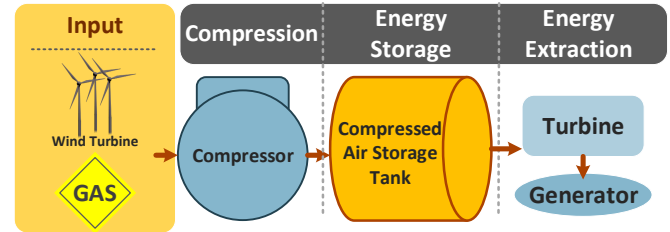


Fig. 2: CAES process based on wind turbine generation

2.3 Structure of EHS

Fig. 3 shows the structure of the EHS consisting of a CHP unit, heat storage system, GB unit, and wind turbine in coordination with P2G storage and tri-CAES system. In the first step, the data regarding electrical, gas, and heat loads, as well as energy prices are collected. Secondary, the hub operator in the form of EHS uses the energy carriers including electricity, gas, and heat in order to reduce somehow the operating cost. In more details, this system is fed by the upstream gas and electricity networks and the wind turbines. The P2G storage, tri-CAES system, and CHP unit are the coupling points between the upstream gas and electricity networks. The optimum operating schedule of P2G storage in coordination with tri-CAES system and other EHS equipment can help system's operator to consider the uncertainties resulting from the wind turbines generation, electricity market price, and energy demands. The outputs of EHS includes meeting the demands of electrical, gas, and thermal in three sectors of residential, commercial, and industrial. In more details, the electrical, heat, and gas demands are described in the following separate parts:

2.3.1 Electrical Demand: As can be seen in Fig. 3, electrical demands are fulfilled by the upstream electricity network, wind turbines, CAES system, and CHP unit. The tri-state CAES system operates in one of the following three modes: (i) charging during low-price periods, (ii) discharging during high-price periods, and (iii) simple cycle gas generator when the reservoir is evacuated or the gas and electricity prices are low and high, respectively. The simple cycle mode can present many economic opportunities for the hub system's operator.

2.3.2 Heat Demand: Heat demand is fulfilled by the district heating network, heat storage system, CHP unit, and GB unit. Mainly, due to heat loss reduction, the district heating networks only meet the local demands of consumers in a local region. It should be pointed out that the converted energy could be utilized to store, for meeting gas demand, and as input fuel for CHP and GB units.

2.3.3 Gas Demand: Gas demand is met by the upstream gas network and P2G storage. Some proportion of the purchased natural gas from the upstream gas network, as well as some of the power generated by P2G, are used in order to supply gas demand. In the time intervals that electricity price is low, P2G storage could effectively convert electrical energy into compatible natural gas.

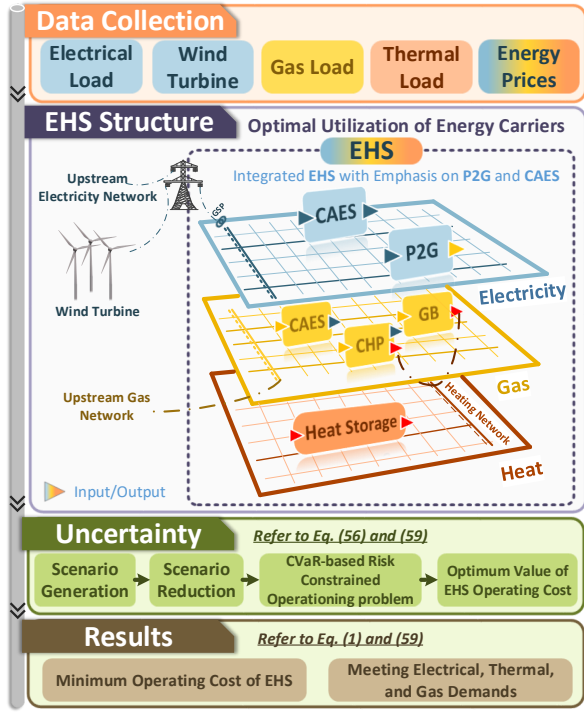


Fig. 3: Schematic for the integrated EHS

3 Problem Formulation

In the day-ahead market, requests for the total hours of the next day are submitted to the day-ahead market at once. Day-ahead market prices for the total hours of the next day are determined at once when the day-ahead market is cleared, then the so-called second level uncertainty associated with the development of the real-time market takes place. So, in this paper, the EHS operator solves a day-ahead scheduling problem before submitting its bids to the day-ahead market in which the uncertainties related to the real-time stage are also modeled. Uncertainties associated with the real-time stage play an important role in sending the demand of the EHS to the energy market. In this section, a mathematical formulation is presented concerning the day-ahead scheduling of the EHS with the coordinated operating of P2G storage and tri-state CAES system in the presence of load shifting program considering the technical constraints of the units. Stochastic objective function has been applied to minimize the total operating cost of the integrated EHS taking into account the uncertainties regarding electricity market price, time-varying generation of the wind turbine, and demands of electrical, gas, and heat. The objective function and constraints of the problem are explained in the following sub-sections.

3.1 Objective Function

The objective function of the proposed model, as demonstrated in Eq. (1), aims at minimizing total operating cost, which contains four mathematical expressions. The first term of the objective function determines the cost incurred and the revenue obtained from purchasing and selling electricity from/to the upstream electricity network. The electricity purchased from the upstream network is used to supply the hourly electrical demands, and given as input to the P2G unit. The second term represents the variable operating and maintenance costs of the CAES unit in charging, discharging, and simple cycle modes. The third term of the objective function is associated to the natural gas purchased to support heat and gas demands, as well as the gas surplus sold to the upstream gas network. Given that the natural gas is utilized as the primary fuel for CHP, GB, and CAES units (in discharging and simple cycle modes), therefore, the operating costs of these units are considered in the third term of the objective function. Finally, the load shifting program cost is

expressed in the fourth term. This term is related to the costs paid to the residential, commercial, and industrial consumers to execute load shifting program.

$$\min \sum_{s=1}^{NS} \pi_s \sum_{t=1}^{NT} \left(\begin{aligned} & \lambda_{t,s}^e EL_{t,s}^+ - \lambda_{t,s}^e EL_{t,s}^- \\ & + \sum_{k=1}^{NK} \left[P_{t,s}^{k,d} VOM^{Exp} + P_{t,s}^{k,si} (VOM^{Exp} + VOM^C) + P_{t,s}^{k,c} VOM^C \right] \\ & + \lambda_{t,s}^g GM_{t,s}^+ - \lambda_{t,s}^g GM_{t,s}^- \\ & + \sum_{m=1}^{NM} Inc_m (dr_{m,t,s}^{dn} + dr_{m,t,s}^{up}) \end{aligned} \right) \quad (1)$$

3.2 Problem Constraints

3.2.1 CHP Unit Constraints: According to the nature of the cogeneration units, the generation of heat and power affects the other generations. To illustrate this dependency, the heat-power feasible operating region of each CHP unit in the proposed integrated EHS is depicted in Fig. 4. To this end, linear equations are applied to describe the operating region of the CHP units, which are formulated by Eqs. (2)-(6). In these equations, indices A, B, C, and D represent the marginal points of the feasible operating region for the CHP unit. Eqs. (2) and (3) ensure that the electricity and heat energy provided by the CHP unit do not exceed their permissible limits. Eq. (4) models the area under the curve AB. Eqs. (5) and (6) model the area under the curve BC and the upper area of curve CD, respectively.

$$P_{t,s}^{i,min} I_{t,s}^i \leq P_{t,s}^i \leq P_{t,s}^{i,max} I_{t,s}^i \quad (2)$$

$$0 \leq H_{t,s}^i \leq H_B^i \times I_{t,s}^i \quad (3)$$

$$P_{t,s}^i - P_A^i - \frac{P_A^i - P_B^i}{H_A^i - H_B^i} \times (H_{t,s}^i - H_A^i) \leq 0 \quad (4)$$

$$P_{t,s}^i - P_B^i - \frac{P_B^i - P_C^i}{H_B^i - H_C^i} \cdot (H_{t,s}^i - H_B^i) \geq (I_{t,s}^i - 1) \cdot M \quad (5)$$

$$P_{t,s}^i - P_C^i - \frac{P_C^i - P_D^i}{H_C^i - H_D^i} \cdot (H_{t,s}^i - H_C^i) \geq (I_{t,s}^i - 1) \cdot M \quad (6)$$

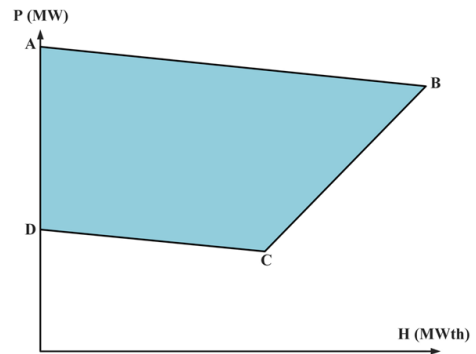


Fig. 4: Feasible operating region of each CHP unit

The limitations of ramping up and down regarding the CHP unit are presented by Eqs. (7)-(10), in which the binary variable is equal to one if each CHP unit is in the ON mode, otherwise it will be zero.

$$P_{t,s}^i - P_{t-1,s}^i \leq (1 - Y_{t,s}^i)R^{i,up} + Y_{t,s}^i P^{i,min} \quad (7)$$

$$P_{t-1,s}^i - P_{t,s}^i \leq (1 - Z_{t,s}^i)R^{i,dn} + Z_{t,s}^i P^{i,min} \quad (8)$$

$$Y_{t,s}^i - Z_{t,s}^i = I_{t,s}^i - I_{t-1,s}^i \quad (9)$$

$$Y_{t,s}^i + Z_{t,s}^i \geq 1 \quad (10)$$

Equations (11)-(14) and (15)-(18) indicate the minimum up time and the minimum down time limits, respectively.

$$UT^i = \max \left\{ 0, \min \left[NT, (T^{i,ON} - X_{(t=0)}^{i,ON})I_{(t=0)}^i \right] \right\} \quad (11)$$

$$\sum_{t=1}^{UT^i} (1 - I_{t,s}^i) = 0 \quad \forall t = 1, \dots, UT^i \quad (12)$$

$$\sum_{j=t}^{t+T^{i,ON}-1} I_{j,s}^i \geq T^{i,ON} Y_{t,s}^i \quad (13)$$

$$\forall t = UT^i + 1, \dots, NT - T^{i,ON} + 1$$

$$\sum_{j=t}^{UT^i} (I_{j,s}^i - Y_{t,s}^i) \geq 0 \quad \forall t = NT - T^{i,ON} + 2, \dots, NT \quad (14)$$

$$DT^i = \max \left\{ 0, \min \left[NT, (T^{i,OFF} - X_{(t=0)}^{i,OFF})(1 - I_{(t=0)}^i) \right] \right\} \quad (15)$$

$$\sum_{t=1}^{DT^i} I_{t,s}^i = 0 \quad \forall t = 1, \dots, DT^i \quad (16)$$

$$\sum_{j=t}^{t+T^{i,OFF}-1} (1 - I_{j,s}^i) \geq T^{i,OFF} Z_{t,s}^i \quad (17)$$

$$\forall t = DT^i + 1, \dots, NT - T^{i,OFF}$$

$$\sum_{j=t}^{DT^i} (1 - I_{j,s}^i - Z_{t,s}^i) \geq 0 \quad \forall t = NT - T^{i,OFF} + 2, \dots, NT \quad (18)$$

Start-up and shut-down fuel consumption of the CHP unit are calculated by Eqs. (19) and (20) as follows:

$$SU_{t,s}^i \geq sug^i (I_{t,s}^i - I_{t-1,s}^i); \quad SU_{t,s}^i \geq 0 \quad (19)$$

$$SD_{t,s}^i \geq sdg^i (I_{t-1,s}^i - I_{t,s}^i); \quad SD_{t,s}^i \geq 0 \quad (20)$$

Equation (21) demonstrates the amount of natural gas consumed by the CHP unit.

$$GC_{t,s}^i = \frac{P_{t,s}^i}{\eta^i} + SU_{t,s}^i + SD_{t,s}^i \quad (21)$$

3.2.2 GB Constraints: The upper and lower levels of GB output for each scenario at any hour of the scheduling horizon are constrained by Eq. (22). In addition, the amount of natural gas consumed by GB with regards to its heat production at any hour is calculated by Eq. (23).

$$H^{b,min} \times I_{t,s}^b \leq H_{t,s}^b \leq H^{b,max} \times I_{t,s}^b \quad (22)$$

$$GB_{t,s}^b = \frac{H_{t,s}^b}{\eta^b} \quad (23)$$

3.2.3 Heat Storage System Constraints: The reserved heat in the heat storage system for each scenario at any hour of the scheduling horizon is expressed by Eq. (24). Furthermore, Eq. (25) ensures that the thermal energy stored in the heat storage does not exceed the reservoir capacity. The ramping up/down rates of the heat storage are indicated by Eqs. (26) and (27), respectively.

$$B_{t,s}^{hs} = (1 - \eta^{hs})B_{t-1,s}^{hs} + H_{t,s}^{hs,c} - H_{t,s}^{hs,d} - \beta_{loss}SU_{t,s}^{hs} + \beta_{gain}SD_{t,s}^{hs} \quad (24)$$

$$B^{hs,min} \leq B_{t,s}^{hs} \leq B^{hs,max} \quad (25)$$

$$B_{t,s}^{hs} - B_{t-1,s}^{hs} \leq B^{hs,c,max} \quad (26)$$

$$B_{t-1,s}^{hs} - B_{t,s}^{hs} \leq B^{hs,d,max} \quad (27)$$

3.2.4 CAES Constraints: Equation (28) prevents the CAES system to be operated simultaneously in three modes of charging, discharging and simple cycle. The upper and lower levels of charging, discharging, and simple cycle modes of the CAES system are expressed by Eqs. (29)-(31).

$$I_{t,s}^{k,c} + I_{t,s}^{k,d} + I_{t,s}^{k,si} \leq 1 \quad (28)$$

$$P^{k,c,min} I_{t,s}^{k,c} \leq P_{t,s}^{k,c} \leq P^{k,c,max} I_{t,s}^{k,c} \quad (29)$$

$$P^{k,d,min} I_{t,s}^{k,d} \leq P_{t,s}^{k,d} \leq P^{k,d,max} I_{t,s}^{k,d} \quad (30)$$

$$P^{k,si,min} I_{t,s}^{k,si} \leq P_{t,s}^{k,si} \leq P^{k,si,max} I_{t,s}^{k,si} \quad (31)$$

Equation (32) indicates that the reserved energy in the CAES in each hour depends on the energy levels in the previous time period, as well as charging and discharging energy. The range of the CAES reservoir is demonstrated by Eq. (33). Moreover, Eq. (34) states that the level of the CAES reservoir at the end of the scheduling must be equal to the initial level of the reservoir.

$$A_{t,s}^k = A_{t-1,s}^k + \eta^{k,c} P_{t,s}^{k,c} - \frac{P_{t,s}^{k,d}}{\eta^{k,d}} \quad (32)$$

$$A^{k,min} \leq A_{t,s}^k \leq A^{k,max} \quad (33)$$

$$A_{0,s}^k = A_{NT,s}^k \quad (34)$$

Equation (35) states the amount of natural gas consumed by CAES in discharging and simple cycle modes. It is worth mentioning that the CAES efficiency during discharge mode is twice the simple cycle mode [33].

$$GK_{t,s}^k = \frac{P_{t,s}^{k,d}}{\eta^{k,d}} + \frac{P_{t,s}^{k,si}}{\eta^{k,si}} \quad (35)$$

3.2.5 P2G Storage Constraints: Converted natural gas by P2G storage can be injected into the upstream gas network or stored in the gas storage, as represented by Eq. (36). Also, the limit on electricity power consumed by the P2G storage is shown in Eq. (37).

$$G_{t,s}^{pg,c} + GE_{t,s}^{pg} = \eta^{pg} P_{t,s}^{pg} \quad (36)$$

$$0 \leq P_{t,s}^{pg} \leq P^{pg,max} \quad (37)$$

The reservoir balance, maximum capacity of injected and stored gas, and reservoir capacity limit of the P2G storage are specified by Eqs. (38)-(42). Similar to other storage units, gas reservoir level at the end of the scheduling period must be equal to the initial level of the reservoir, which is stated as Eq. (42).

$$V_{t,s}^{pg} = V_{t-1,s}^{pg} + G_{t,s}^{pg,c} - G_{t,s}^{pg,d} \quad (38)$$

$$0 \leq G_{t,s}^{pg,c} \leq G^{pg,c,max} \quad (39)$$

$$0 \leq G_{t,s}^{pg,d} \leq G^{pg,d,max} \quad (40)$$

$$V_{t,s}^{pg,min} \leq V_{t,s}^{pg} \leq V^{pg,max} \quad (41)$$

$$V_{0,s}^{pg} = V_{NT,s}^{pg} \quad (42)$$

3.2.6 Upstream Gas and Electricity Networks Constraints: The constraints of the electricity and natural gas exchange between the integrated EHS, the upstream gas and electricity networks are shown in Eqs. (43)-(48). The binary variables are used to prevent the transmission and receipt of electricity and gas at the same time.

$$0 \leq EL_{t,s}^+ \leq PL^{B,max} e_{t,s}^+ \quad (43)$$

$$0 \leq EL_{t,s}^- \leq PL^{S,max} e_{t,s}^- \quad (44)$$

$$e_{t,s}^+ + e_{t,s}^- \leq 1 \quad (45)$$

$$0 \leq GM_{t,s}^+ \leq GT^{B,max} g_{t,s}^+ \quad (46)$$

$$0 \leq GM_{t,s}^- \leq GT^{S,max} g_{t,s}^- \quad (47)$$

$$g_{t,s}^+ + g_{t,s}^- \leq 1 \quad (48)$$

3.2.7 Multiple Load Shifting Constraints: The load shifting program is applied as one of the most effective methods of DSM technique to manage the electrical demands. Electrical demands consist of three components including residential, commercial, and industrial demands. To increase the customers' satisfaction, the load shifting program is utilized considering the multiple electrical loads' activity schedule. According to Eqs. (49) and (50), electrical demands of the EHS will be shifted from peak periods into the valley and off-peak periods concerning the participation rate of consumers and its activity schedule. Besides, the amount of variation in the first electrical load profile during the 24 hours horizon should be equal to zero, which is shown in Eq. (51).

$$0 \leq dr_{m,t,s}^{up} \leq DR_{m,t} \times DL_{t,s} \quad (49)$$

$$0 \leq dr_{m,t,s}^{dn} \leq DR_{m,t} \times DL_{t,s} \quad (50)$$

$$\sum_{t=t_m}^{NT_m} dr_{m,t,s}^{up} = \sum_{t=t_m}^{NT_m} dr_{m,t,s}^{dn} \quad (51)$$

Eventually, the final demand profile of each sector is presented as follows:

$$d_{t,s}^{DR} = DL_{t,s} + dr_{m,t,s}^{up} - dr_{m,t,s}^{dn} \quad (52)$$

3.2.8 Multi-energy Balance Constraints: Equations (53)-(55) depict that each type of primary energy generated by the upstream networks plus the components of EHS must satisfy each type of demand, for each scenario at any hour of the scheduling horizon.

$$EL_{t,s}^+ - EL_{t,s}^- + \sum_{i=1}^{NI} P_{t,s}^i + PW_{t,s} - P_{t,s}^{pg} + \sum_{k=1}^{NK} (P_{t,s}^{k,si} + P_{t,s}^{k,d} - P_{t,s}^{k,c}) = d_{t,s}^{DR} \quad (53)$$

$$GM_{t,s}^+ - GM_{t,s}^- + GE_{t,s}^{pg} + G_{t,s}^{pg,d} - \sum_{i=1}^{NI} GC_{t,s}^i - \sum_{k=1}^{NK} GK_{t,s}^k - \sum_{b=1}^{NB} GB_{t,s}^b = GL_{t,s} \quad (54)$$

$$\sum_{i=1}^{NI} H_{t,s}^i + \sum_{b=1}^{NB} H_{t,s}^b + \sum_{h=1}^{NHS} (H_{t,s}^{h,s,d} - H_{t,s}^{h,s,c}) = HL_{t,s} \quad (55)$$

3.3 CVaR-based Risk Measurement

In this paper, the risk of operating cost variability is modeled by the Conditional Value-at-Risk (CVaR) for a confidence level α . The CVaR is approximated by the operating cost of the $(1 - \alpha) \times 100\%$ scenarios with the highest operating cost. The CVaR is calculated by solving the following optimization problem:

$$CVaR = \min_{VaR, \eta_s} VaR + \frac{1}{1 - \alpha} \sum_{s=1}^{NS} \pi_s \eta_s \quad (56)$$

$$\left[\sum_{t=1}^{NT} \left(\begin{aligned} &\lambda_{t,s}^e EL_{t,s}^+ - \lambda_{t,s}^e EL_{t,s}^- \\ &+ \sum_{k=1}^{NK} \left[P_{t,s}^{k,d} VOM^{Exp} + P_{t,s}^{k,si} (VOM^{exp} + VOM^C) \right. \right. \\ &\quad \left. \left. + P_{t,s}^{k,c} VOM^C \right] \right. \\ &+ \lambda_{t,s}^g GM_{t,s}^+ - \lambda_{t,s}^g GM_{t,s}^- \\ &+ \sum_{m=1}^{NM} Inc_m dr_{m,t,s}^{dn} + \sum_{m=1}^{NM} Inc_m dr_{m,t,s}^{up} \end{aligned} \right) \right] - VaR \leq \eta_s \quad (57)$$

$$\eta_s \geq 0 \quad (58)$$

For a given α in the open interval (0,1), VaR demonstrates the cheapest operating cost, as well as guaranteeing that the probability of achieving a total operating cost higher than the cheapest operating cost is lower than $(1 - \alpha)$. Besides, η_s is the difference between the operating cost in each scenario and VaR if the difference is positive; otherwise, it equals to zero. Hence, considering CVaR-based risk, the problem is formulated as follow:

$$\min (1 - \beta) \sum_{s=1}^{NS} \pi_s \left[\sum_{t=1}^{NT} \left(\begin{aligned} &\lambda_{t,s}^e EL_{t,s}^+ - \lambda_{t,s}^e EL_{t,s}^- \\ &+ \sum_{k=1}^{NK} \left[P_{t,s}^{k,d} VOM^{Exp} + P_{t,s}^{k,si} (VOM^{exp} + VOM^C) \right. \right. \\ &\quad \left. \left. + P_{t,s}^{k,c} VOM^C \right] \right. \\ &+ \lambda_{t,s}^g GM_{t,s}^+ - \lambda_{t,s}^g GM_{t,s}^- \\ &+ \sum_{m=1}^{NM} Inc_m dr_{m,t,s}^{dn} + \sum_{m=1}^{NM} Inc_m dr_{m,t,s}^{up} \end{aligned} \right) \right] + \beta \left(\zeta + \frac{1}{1 - \alpha} \sum_{s=1}^{NS} \pi_s \eta_s \right) \quad (59)$$

It should be pointed out that, in this section, all constraints are similar to Eqs. (2)-(52), as well as Eqs. (57) and (58).

4 Results and Discussion

The proposed model for the EHS in coordination with P2G storage and CAES system is a Mixed Integer Programming (MIP). Computer simulations were performed by GAMS software, CPLEX solver, running on a personal computer with a 2.4 GHz CPU with 6 Gigabytes of memory.

To evaluate the proposed model, the considered EHS includes a CHP, a GB, a wind farm, a heat storage system, a CAES, and a P2G storage system to supply the electrical, thermal and gas loads. The parameters of the EHS are indicated in Tables (1)-(5). The load profile regarding electrical, thermal, gas and wind farm is shown in Fig. 5. Also, the prices of the electricity market and natural gas are depicted in Fig. 6. The nominated wind farm capacity is 50 MW. The forecasted wind power is shown in Fig. 7. Monte Carlo Simulation has been applied in order to model the uncertainties associated with electrical, thermal and gas loads, as well as wind turbine and electricity prices. It should be noted that electrical, thermal and gas loads, as well as wind turbine and electricity prices follow a normal distribution function with deviations of 5, 5, 5, 15 and 10 percent, respectively.

Table 1 Efficiency of the HUB

| Parameter | Value |
|---------------|-------|
| η^i | 0.35 |
| η^b | 0.8 |
| η^{hs} | 0.9 |
| η^{pg} | 0.75 |
| $\eta^{k,c}$ | 0.9 |
| $\eta^{k,d}$ | 0.9 |
| $\eta^{k,si}$ | 0.4 |

Table 2 Characteristics of CHP unit

| Parameter | Value |
|--------------------|-------|
| $P^{i,min}(MW)$ | 48 |
| $P^{i,max}(MW)$ | 105 |
| $H^{i,min}(MWth)$ | 0 |
| $H^{i,max}(MWth)$ | 87 |
| Initial Status (h) | 1 |
| Min Down (h) | 1 |
| Min Up (h) | 1 |
| Ramp (MW/h) | 55 |

Table 3 Heat storage system parameters

| Parameter | Value |
|---------------------|-------|
| $B^{hs,min}(MWh)$ | 0 |
| $B^{hs,max}(MWh)$ | 60 |
| $B^{hs,d,max}(MWh)$ | 20 |
| $B^{hs,c,max}(MWh)$ | 20 |

To evaluate the proposed model, the following four cases are considered:

Table 4 P2G storage system parameters

| Parameter | Value |
|--------------------|-------|
| $V^{pg,min}(MWh)$ | 50 |
| $V^{pg,max}(MWh)$ | 180 |
| $G^{pg,d,max}(MW)$ | 40 |
| $G^{pg,c,max}(MW)$ | 40 |
| $P^{pg,max}(MW)$ | 50 |

Table 5 CAES system parameters

| Parameter | Value |
|--------------------|-------|
| $A^{k,min}(MWh)$ | 50 |
| $A^{k,max}(MWh)$ | 350 |
| $P^{k,d,min}(MW)$ | 5 |
| $P^{k,d,max}(MW)$ | 50 |
| $P^{k,c,min}(MW)$ | 5 |
| $P^{k,c,max}(MW)$ | 50 |
| $P^{k,si,min}(MW)$ | 5 |
| $P^{k,si,max}(MW)$ | 50 |

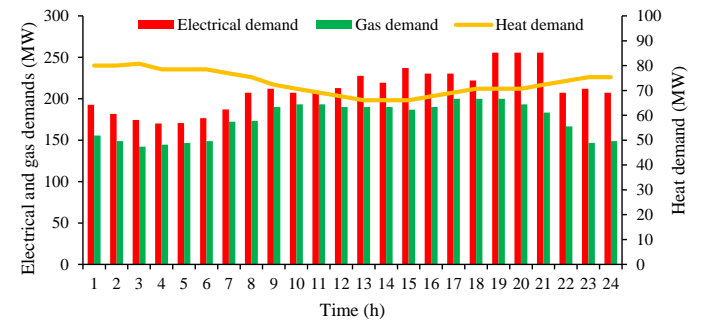


Fig. 5: Predicted data for hourly electricity, heat and natural gas demands

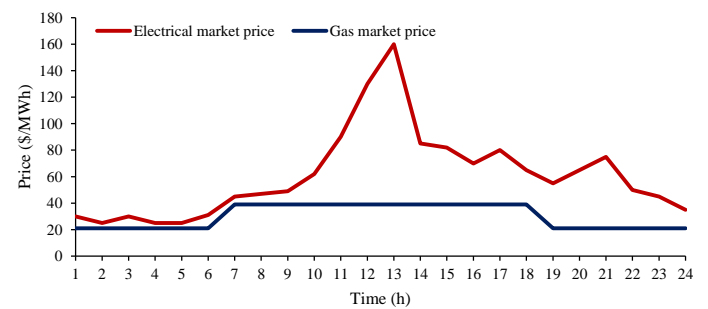


Fig. 6: Predicted data for hourly prices of electricity and gas

4.1 Case 1: Solving the problem with CAES and without considering uncertainty

In this case, the effect of the integration of the CAES system on EHS is investigated. Fig. 8 shows the hourly scheduling of the CAES system. As it is shown, the hub operator purchases electricity from the upstream network/utility grid in times when the electricity prices are low and stores it in the CAES system as compressed air. Then, in times of high electricity prices, instead of purchasing power from the upstream network, the energy stored in the CAES system is used to supply its consumption load. Also, since the CAES system has three

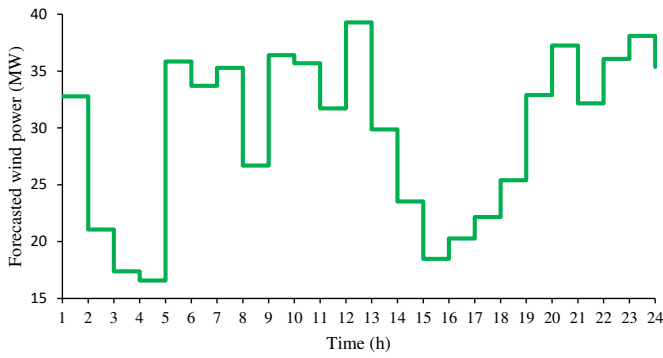


Fig. 7: Forecasted wind power

active modes, the hub operator at hours 19, 20, and 21 when the electricity price is average, purchases power from the CAES system in the simple cycle mode. Fig. 9 depicts the impact of the CAES system on the power purchased from the upstream network in both non-CAES and CAES modes. As can be seen, during the hours when the CAES system is in charge, the amount of purchased power from the upstream network has increased and vice versa. In addition to this, Fig. 10 shows the effect of considering the CAES system on the gas purchased from the upstream network in two non-CAES and CAES modes. The amount of gas purchased from the upstream network has increased in the presence of the storage system, which increases the dependence of the EHS on natural gas. Table 6 indicates the impact of the CAES system on the total operating cost considering the CAES system with three active modes. As can be seen, while the purchased gas from the grid has increased, the purchasing power has decreased. It has led to reduction in the total operating cost of hub EHS compared to non-CAES and CAES modes with two active modes (regardless of the simple cycle mode).

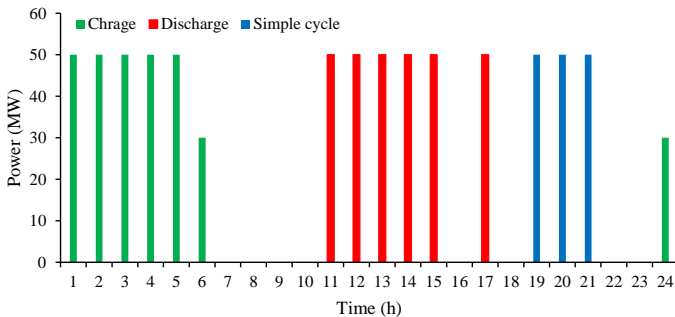


Fig. 8: Hourly Scheduling of CAES system

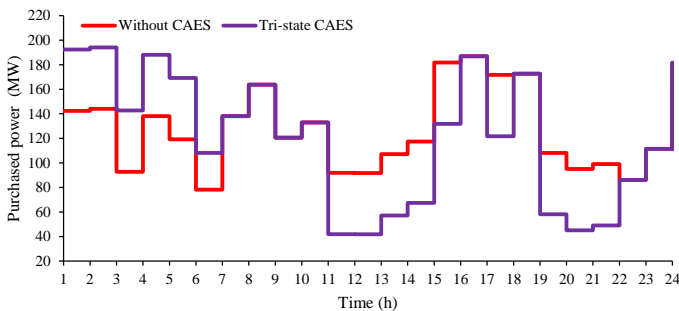


Fig. 9: The effect of CAES with three active modes on the electricity purchased from the electricity market

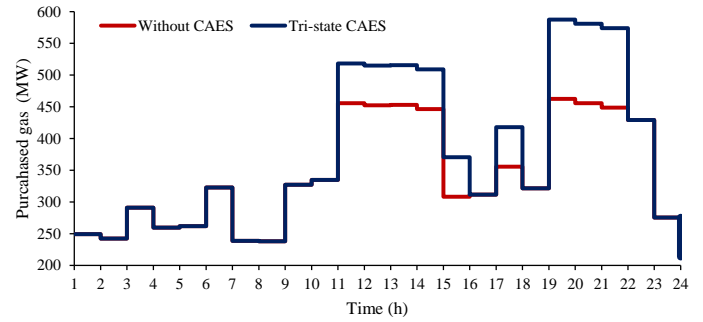


Fig. 10: The effect of CAES with three active modes on the gas purchased from the gas market

Table 6 The effect of CAES on the operating cost of EHS

| | Without CAES | With bi-state CAES | With tri-state CAES |
|---------------------------|--------------|--------------------|---------------------|
| Gas operating cost (\$) | 247666.23 | 260041.23 | 270166.23 |
| Power operating cost (\$) | 180739.05 | 158669.05 | 147819.05 |
| Total operating cost (\$) | 428405.27 | 418710.27 | 417985.27 |

4.2 Case 2: Case 1 with P2G system

In this case, the effect of integrating the P2G storage system into EHS with the presence of the CAES system is discussed. Fig. 11 explains how P2G is scheduled by the hub operator. In times of low electricity prices, the hub operator buys electricity from the upstream network and converts it into natural gas by P2G technology. The produced natural gas is stored in the storage system to be used when the gas price is high. It should be noted that the storage system in $t = 24$ is also in the charge mode due to the initial and final values of the energy stored in the gas storage should be equal. In the time intervals between 7-9 and 12-13, the hub operator makes the use of gas stored in the storage system instead of purchasing natural gas from the upstream network to supply its gas loads. Fig. 12 states the impact of P2G storage on the gas and electricity purchased from the upstream network compared to case 1. As it can be seen, in the early hours when the storage is in charge, the power purchased from the upstream network has increased, and the amount of gas purchased from the upstream network has decreased during discharge mode. Table 7 indicates the effect of considering simultaneously the P2G storage and the CAES system in the EHS. It has led to a reduction in the total amount of purchased gas and electricity, which confirms the advantages of taking into account these two technologies simultaneously in the EHS.

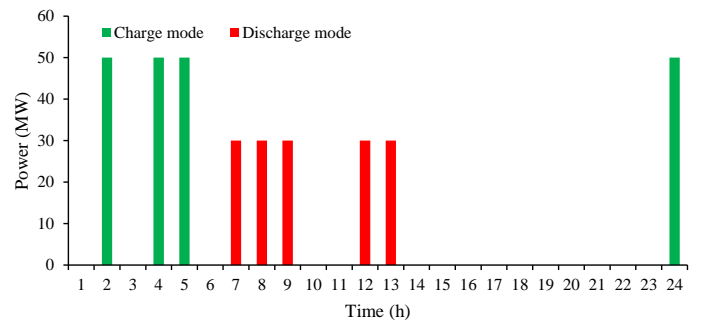


Fig. 11: Hourly scheduling of P2G storage system

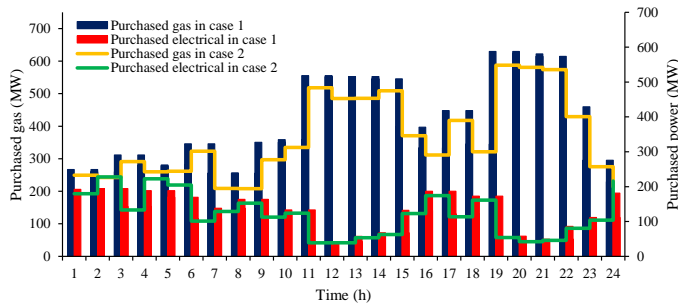


Fig. 12: The effect of P2G on the power and gas purchased from the upstream network

Table 7 The effect of P2G on the operating cost of EHS

| | With Tri-state CAES | Tri-state CAES+P2G storage |
|---------------------------|---------------------|----------------------------|
| Gas operating cost (\$) | 270166.227 | 264316.227 |
| Power operating cost (\$) | 147819.048 | 152619.047 |
| Total operating cost (\$) | 417985.274 | 416935.274 |

4.3 Case 3: Case 2 with multiple loads

In this case, the impact of multiple shiftable loads on EHS is investigated. 10% of the load is considered as a shiftable, which includes 5% of industrial, 3% of commercial, and 2% of the residential loads. The active mode of each shiftable load is given in [34]. Fig. 13 demonstrates the consequence of multiple shiftable loads on the electrical load profile of the energy hub. As it can be seen, in this case, loads of each industrial, commercial and residential sector, depending on their active mode, have shifted from the hours with high electricity prices to the hours with low electricity prices. It ultimately led to purchasing less amount of power by hub operator in hours with high prices. Therefore, the operating cost of the EHS has dropped to \$ 409817.261 in comparison with case 2. Moreover, the effect of the participation rate of multiple shiftable loads on the operating cost of EHS is shown in Table 8. As can be seen, with increasing the participation coefficient of shiftable loads, the operating cost of EHS decreases, which is due to the decrease in purchasing electricity from the upstream network in high-cost hours.

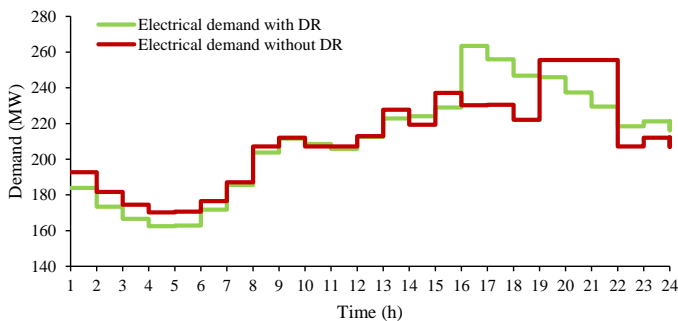


Fig. 13: The effect of multiple shiftable loads on the EHS

4.4 Case 4: Solving the risk-based stochastic problem by taking into account the uncertainties of cases 1 to 3.

This case considers the uncertainty of EHS derived from electrical, gas and thermal loads, electricity price, and the output power of the wind turbine. For this purpose, one thousand scenarios have been generated using the Monte Carlo simulation. Then, this number was

Table 8 the effect of the participation rate of multiple shiftable loads on the operating cost of EHS

| Shiftable load (%) | Total operating cost (\$) |
|--------------------|---------------------------|
| 10 | 409817.26 |
| 12 | 408169.04 |
| 14 | 406520.83 |
| 16 | 404872.61 |
| 18 | 403253.43 |
| 20 | 401814.37 |

reduced to ten scenarios by using the SCENRED GAMS tool. Table 9 shows the probability of occurrence for each scenario. Table 10 describes the expected operating cost under $\beta = 0$ for cases 1 to 3. It should be pointed out, in all three cases, the expected operating cost is higher than its predetermined value. Also, Table 11 states the effect of β variations on the operating cost of EHS, CVAR, and VAR for constant values of $\alpha = 0.9$. In this paper, CVAR is defined as the expected operating cost in the top ten scenarios with the highest operating cost. As can be seen, when β has a direct relationship with the expected operating cost. In fact, higher operating costs occur at a lower risk level, and lower operating costs happen at a higher risk level. Hence, with an increase in β , the hub operator applies a more conservative strategy with lower risk levels, which leads to augmenting the operating cost of the energy hub. Furthermore, with the increase of β , due to applying a risk-averse approach, the expected operating cost in 10% of the scenarios having the highest operating cost will be reduced.

Table 9 Probability of each scenario

| Scenarios | Probability |
|-----------|-------------|
| S1 | 0.082 |
| S2 | 0.132 |
| S3 | 0.062 |
| S4 | 0.188 |
| S5 | 0.018 |
| S6 | 0.205 |
| S7 | 0.014 |
| S8 | 0.078 |
| S9 | 0.182 |
| S10 | 0.039 |

Table 10 The expected operating cost of EHS considering the uncertainties of Case 1 to 3

| | Case 1 | Case 2 | Case 3 |
|------------------------------------|-----------|-----------|-----------|
| Expected gas operating cost (\$) | 266868.77 | 263999.15 | 263999.15 |
| Expected power operating cost (\$) | 150408.86 | 152054.11 | 144802.26 |
| Expected total operating cost (\$) | 417277.63 | 416053.26 | 408801.41 |

Table 11 The effect of increasing the beta coefficient on total operating cost, VaR, and CVaR

| β | Total operating cost (\$) | VaR | CVaR |
|---------|---------------------------|-----------|-----------|
| 0.1 | 408840.85 | 422025.36 | 434767.15 |
| 0.3 | 408895.1 | 422010.33 | 434495.95 |
| 0.5 | 409195.05 | 421948.47 | 434195.56 |
| 0.7 | 409595.11 | 421748.95 | 433895.88 |
| 0.9 | 409695.03 | 421320.15 | 433464.57 |

5 Conclusion

This paper proposed a risk-constrained EHS integrated with the P2G storage and CAES systems, with the presence of multiple shiftable loads. Monte Carlo simulation method was applied to estimate the uncertainties concerning the electrical, thermal and gas loads, wind turbine, and electricity prices. Also, the CVaR-based risk measurement was utilized to manage system uncertainties under a conservative approach. The results indicated that by increasing β , the hub operator would apply a more risk-averse strategy with a higher operating cost. The impacts of considering the P2G and CAES, and multiple shiftable loads can be summarized as follows:

(i) Taking into account the CAES storage in EHS has led to an increase and a decrease the operating costs of gas and electricity, respectively. All in all, it reduces the operating cost of EHS. Considering this technology, along with its benefits, it will raise the dependence of EHS on the natural gas price.

(ii) Considering P2G technology, along with the CAES storage system, has led to a reduction in gas costs as well as the total operating cost of EHS. Therefore, it can compensate for the CAES system problem resulting from the increase in the natural gas costs.

(iii) Considering the multiple shiftable loads along with the P2G and CAES technologies have resulted in a reduction in the amount of electricity purchased from the upstream network. Hence, it has led to enhanced flexibility and dependency of EHS.

In future researches will be focused on the regional-district co-optimization of integrated power, gas and heating systems. In addition, the constraints of the natural gas networks at the transmission level and district heating system will be fully considered. On the other hand, integrated demand response as a novel concept of DRPs is important to be researched for coordinated energy systems.

6 References

- Xu, Y., Ding, T., Ming, Q., Du, P.: 'Adaptive dynamic programming based gas-power network constrained unit commitment to accommodate renewable energy with combined-cycle units', *IEEE Trans. Sustain. Energy*, Early Access
- Ding, T., Hu, Y., Bie, Z.: 'Multi-stage stochastic programming with nonanticipativity constraints for expansion of combined power and natural gas systems', *IEEE Trans. Power Syst.*, 2018, **33**, (1), pp. 317-328
- Ding, T., Xu, Y., Yang, Y., Li, Z., Zhang, X., Blaabjerg, F.: 'A tight linear program for feasibility check and solutions to natural gas flow equations', *IEEE Trans. Power Syst.*, 2019, **34**, (3), pp. 2441-2444
- Ding, T., Xu, Y., Wei, W., Wu, L.: 'Energy flow optimization for integrated power-gas generation and transmission systems', *IEEE Trans. Ind. Inf.*, 2020, **16**, (3), pp. 1677-1687
- Ghanaee, R., Akbari Foroud, A.: 'Economic analysis and optimal capacity sizing of turbo-expander-based microgrid', *IET Renew. Power Gener.*, 2017, **11**, (4), pp. 511-520
- Wang, C., Wei, W., Wang, J., Wu, L., Liang, Y.: 'Equilibrium of interdependent gas and electricity markets with marginal price based bilateral energy trading', *IEEE Trans. Power Syst.*, 2018, **33**, (5), pp. 4854-4867
- Mirzaei, M.A., Sadeghi-Yazdankhah, A., Mohammadi-Ivatloo, B., Marzband, M., Shafie-khah, M., Catal  o, J.P.S.: 'Integration of emerging resources in IGDT-based robust scheduling of combined power and natural gas systems considering flexible ramping products', *Energy*, 2019, **189**, pp. 116195
- Vogelin, P., Georges, G., Boulouchos, K.: 'Design analysis of gas engine combined heat and power plants (CHP) for building and industry heat demand under varying price structures', *Energy*, 2017, **125**, pp. 356-366
- Nazari-Heris, M., Mirzaei, M.A., Mohammadi-Ivatloo, B., Marzband, M., and Asadi, S.: 'Economic-environmental effect of power to gas technology in coupled electricity and gas systems with price-responsive shiftable loads', *J. Clean. Prod.*, 2020, **244**, pp. 118769
- Jadidbonab, M., Mousavi-Sarabi, H., Mohammadi-Ivatloo, B.: 'Risk-constrained scheduling of solar-based three state compressed air energy storage with waste thermal recovery unit in the thermal energy market environment', *IET Renew. Power Gener.*, 2019, **13**, (6), pp. 920-929
- Chen, S., Wei, Z., Sun, G., Wang, D., Zang, H.: 'Steady state and transient simulation for electricity-gas integrated energy systems by using convex optimisation', *IET Gener. Transm. Distrib.*, 2018, **12**, (9), pp. 2199-2206
- Clegg, S., Mancarella, P.: 'Storing renewables in the gas network: modelling of power-to-gas seasonal storage flexibility in low carbon power systems', *IET Gener. Transm. Distrib.*, 2016, **10**, (3), pp. 566-575
- Zeng, Z., Ding, T., Xu, Y., Yang, Y., and Dong, Z.: 'Reliability evaluation for integrated power-gas systems with power-to-gas and gas storages', *IEEE Trans. Power Syst.*, 2020, **35**, (1), pp. 571-583
- Shams, M., Shahabi, M., Khodayar, M.: 'Stochastic day-ahead scheduling of multiple energy carrier microgrids with demand response', *Energy*, 2018, **155**, pp. 326-338
- Aliasghari, P., Zamani-Gargari, M., Mohammadi-Ivatloo, B.: 'Look-ahead risk-constrained scheduling of wind power integrated system with compressed air energy storage (CAES) plant', *Energy*, 2018, **160**, pp. 668-677
- Jadidbonab, M., Dolatabadi, A., Mohammadi-Ivatloo, B., Abapour, M., Asadi, S.: 'Risk-constrained energy management of PV integrated smart energy hub in the presence of demand response program and compressed air energy', *IET Renew. Power Gener.*, 2019, **13**, (6), pp. 998-1008
- Pazouki, S., Haghifam, M.R.: 'Optimal planning and scheduling of energy hub in presence of wind, storage and demand response under uncertainty', *Electr. Power Energy Syst.*, 2016, **80**, pp. 219-239
- Massrur, H.R., Niknam, T., Fotuhi-Firuzabad, M.: 'Investigation of carrier demand response uncertainty on energy flow of renewable-based integrated electricity-gas-heat systems', *IEEE Trans. Ind. Inf.*, 2018, **14**, (11), pp. 5133-5142
- Gerami Moghaddam, I., Saniei, M., Mashhour, E.: 'A comprehensive model for self-scheduling an energy hub to supply cooling, heating and electrical demands of a building', *Energy*, 2016, **94**, pp. 157-170
- Alipour, M., Zare, K., Abapour, M.: 'MINLP probabilistic scheduling model for demand response programs integrated energy hubs', *IEEE Trans. Ind. Inf.*, 2018, **14**, (1), pp. 79-88
- Majidi, M., Nojavan, S., Zare, K.: 'A cost-emission framework for hub energy system under demand response program', *Energy*, 2017, **134**, pp. 157-166
- Huo, D., Le Blond, S., Gu, C., Wei, W., Yu, D.: 'Optimal operation of interconnected energy hubs by using decomposed hybrid particle swarm and interior-point approach', *Int. J. Electr. Power Energy Syst.*, 2018, **95**, pp. 36-46
- Dolatabadi, A., Mohammadi-ivatloo, B., Abapour, M., Tohidi, S.: 'Optimal stochastic design of wind integrated energy hub', *IEEE Trans. Ind. Inf.*, 2017, **13**, (5), pp. 2379-2388
- Dolatabadi, A., Jadidbonab, M., Mohammadi-Ivatloo, B.: 'Short-term scheduling strategy for wind-based energy hub: A hybrid stochastic/IGDT approach', *IEEE Trans. Sustainable Energy*, 2019, **10**, (1), pp. 438-448
- Ma, T., Wu, J., Hao, L.: 'Energy flow modeling and optimal operation analysis of the micro energy grid based on energy hub', *Energy Convers. Manage.*, 2017, **133**, pp. 292-306
- Roldan-Blay, C., Escrive, G.E., Roldan-Porta, C., Alvarez-Bel, C.: 'An optimisation algorithm for distributed energy resources management in micro-scale energy hubs', *Energy*, 2017, **132**, pp. 126-135
- Vahid-Pakdel, M.J., Nojavan, S., Mohammadi-Ivatloo, B., Zare, K.: 'Stochastic optimization of energy hub operation with consideration of thermal energy market and demand response', *Energy Convers. Manage.*, 2017, **145**, pp. 117-128
- Dolatabadi, A., Mohammadi-Ivatloo, B.: 'Stochastic risk-constrained scheduling of smart energy hub in the presence of wind power and demand response', *Appl. Therm. Eng.*, 2017, **123**, pp. 40-49
- Pazouki, S., Haghifam, M.R., Moser, A.: 'Uncertainty modeling in optimal operation of energy hub in presence of wind, storage and demand response', *Int. J. Electr. Power Energy Syst.*, 2014, **61**, pp. 335-345
- HELMETH: Integrated High-Temperature Electrolysis and Methanation for Effective Power to Gas Conversion. Available at: <http://www.helmeth.eu/index.php/project> [accessed July 10, 2019].
- Soltani, Z., Ghaljehei, G.B., Gharehpajian, M., Aalami, H.A.: 'Integration of smart grid technologies in stochastic multi-objective unit commitment: An economic emission analysis', *Int. J. Electr. Power Energy Syst.*, 2017, **100**, 2018, pp. 565-590
- Mirzaei, M.A., Sadeghi Yazdankhah, A., Mohammadi-Ivatloo, B., Marzband, M., Shafie-khah, M., Catal  o, J.P.S.: 'Stochastic network-constrained co-optimization of energy and reserve products in renewable energy integrated power and gas networks with energy storage system', *J. Clean. Prod.*, 2019, **223**, 2018, pp. 747-758
- Safaei, H., Keith, D.W.: 'Compressed air energy storage with waste heat export: An Alberta case study', *Energy Convers. Manage.*, 2014, **78**, pp. 114-124

- 34 Zare Oskouei, M., Sadeghi Yazdankhah, A.: ‘The role of coordinated load shifting and frequency-based pricing strategies in maximizing hybrid system profit’, *Energy*, 2017, **135**, pp. 370-381